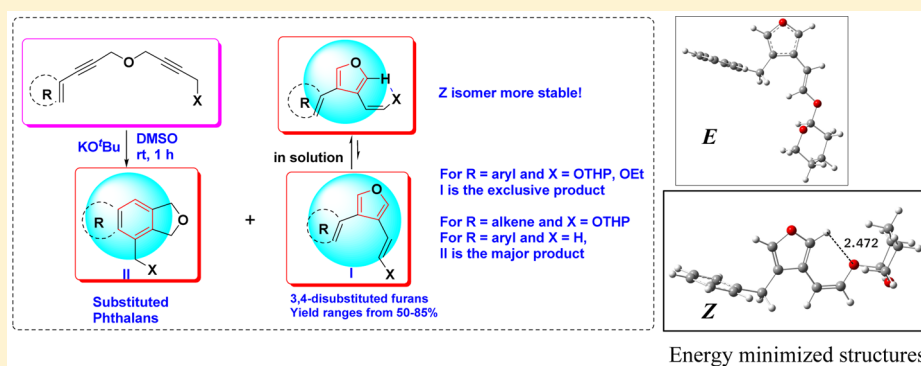


Shifting the Reactivity of Bis-propargyl Ethers from Garratt–Braverman Cyclization Mode to 1,5-H Shift Pathway To Yield 3,4-Disubstituted Furans: A Combined Experimental and Computational Study

Joyee Das,[†] Eshani Das,[‡] Saibal Jana, Partha Sarathi Addy, Anakuthil Anoop,* and Amit Basak*

Department of Chemistry, Indian Institute of Technology Kharagpur, Kharagpur 721 302, India

S Supporting Information

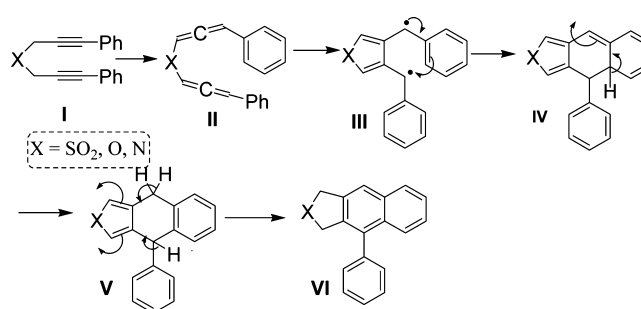


ABSTRACT: Aryl or vinyl substituted bis-propargyl ethers upon base treatment generally form phthalans via the Garratt–Braverman (GB) cyclization pathway. In a major departure from this usual route, several aryl/vinyl bis-propargyl ethers with one of the acetylenic arms ending up with 2-tetrahydropyran-2-yl methyl or ethoxy methyl have been shown to follow the alternative intramolecular 1,5-H shift pathway upon base treatment. The reaction has led to the formation of synthetically as well as biologically important 3,4-disubstituted furan derivatives in good yields. The initially formed *E* isomer in solution (CDCl_3) slowly isomerizes to the *Z* isomer, indicating greater stability of the latter. The factors affecting the interplay between the 1,5-H shift and GB rearrangement have also been evaluated, and the results are supported by DFT-based computational study.

INTRODUCTION

The study of reactivity of bis-propargyl sulfones, ethers, and sulfonamides has drawn interest in recent years.¹ The reaction involves the formation of two C–C bonds in high yields under mild conditions, leading to the formation of an aromatic ring and is popularly known as Garratt–Braverman (GB) cyclization.² The synthetic utility of the reaction has recently been elaborated in a series of publications.³ The involvement of a diradical intermediate from an *in situ* generated bis-allene intermediate (Scheme 1), as proposed initially by Garratt and Braverman⁴ and later supported by computations and selectivity profiles,⁵ is the generally accepted mechanism, although other possibilities like an anionic intramolecular Diels–Alder reaction has also been proposed.⁶ One interesting aspect of the reactivity of appropriately substituted bis-propargyl systems is the possibility of a 1,5-H shift to internally quench the diradical intermediate (Scheme 2). Normally, this reaction occurs when there is no involvement of a double bond (from an alkene or an existing aromatic ring). For systems where this participation is possible, the GB cyclization pathway becomes dominant as that creates a stabilized aromatic ring. It is thus a challenge to shift the reaction toward the 1,5-H shift

Scheme 1. GB Cyclization of Aryl Substituted Bis-propargyl Systems

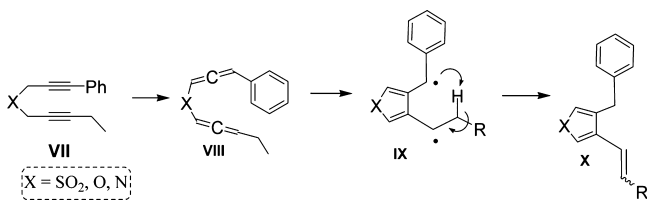


pathway, which creates a lesser stabilized furan system. We have undertaken a project to study the parameters that might help in tilting the preference from GB to 1,5-H shift pathway. The present study has been restricted to bis-propargyl ether systems only as, in these cases, we have achieved a fair amount of

Received: September 25, 2015

Published: December 16, 2015

Scheme 2. 1,5-H Shift from the Diradical Intermediate



success in inducing predominant 1,5-shift, and the results are described herein. Incidentally, the 1,5-H shift products are 3,4-disubstituted furans, which are important in organic synthesis⁷ and are also present in various biologically interesting natural products.⁸ Our method offers an alternative way to obtain these disubstituted furans in high yields.

It was realized that, to offset the participation of the double bond for the GB cyclization, we may need to weaken the C–H bond involved in the 1,5-shift. Another possible strategy may involve the use of different aryl systems with varying degrees of resonance stability or double bond fixation. The latter is important because, in the process of generating an aromatic system in GB cyclization, the pre-existing aromatic ring has to lose its aromaticity to participate in the mutual quenching of diradicals. Higher loss may shift the preference toward the 1,5-shift pathway. These possibilities are schematically represented in Figure 1.

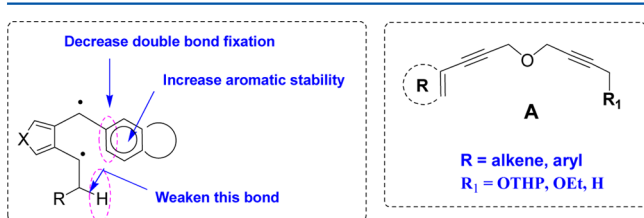


Figure 1. Strategies to tilt the preference toward 1,5 H-shift pathway.

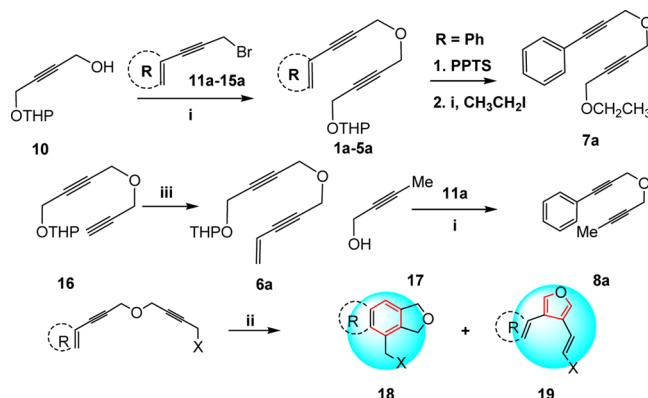
Taking all of these aspects into consideration, we decided to synthesize bis-propargyl ethers as represented by the general structure A (Figure 1). The R group at one arm was planned to be varied from phenyl (or substituted phenyl) to naphthalene or even to a simple alkene. This will provide us with an idea about the influence of electron delocalization on the course of the reaction. At the other end, an ethereal system (OTHP or OEt) was incorporated with the hope that the incipient radical generated during H migration would be stabilized by electron donation from the adjacent oxygen.

RESULTS AND DISCUSSION

The synthesis of the target molecules 1a–8a is shown in Scheme 3 (for 9a, see ref 3d). The key step involved O-alkylation of mono-THP-protected butyne 1,4-diol 10 with the enyne bromides 11a–15a (prepared via enyne coupling and functional group manipulations following published procedures¹). The olefinic substrate 6a was obtained via Sonogashira coupling between the alkyne 16 and vinyl bromide.

The substrates were then subjected to the conditions usually adapted for GB cyclization. Thus, a DMSO solution of the ethers was treated with KO^tBu (1.2 equiv), and the solution was stirred at room temperature for 1 h, by which time all the starting material was consumed. Usual work up (quenching with NH₄Cl and extracting into ethyl acetate), followed by

Scheme 3. Synthesis of Target Propargyl Ethers



For 1a,11a R = Phenyl For 2a,12a R = 2,4-Dimethoxy Phenyl For 3a,13a R = 4-Methoxy Phenyl For 4a,14a R = 4-Methyl Phenyl For 5a, 15a R = Naphthyl

For 1a, 2a, 3a, 4a, 7a H-shift product (19) is exclusive
For 8a GB product (18) is only product
For 5a, 19 is major product
For 6a, 18 is major product

i) NaH, dry DMF, 0 °C to rt, ii) KO^tBu, dry DMSO, rt
iii) Vinyl bromide, PdCl₂(PPh₃)₂, CuI, dry Et₃N, rt

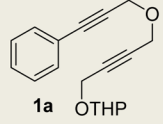
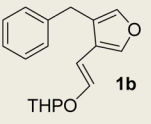
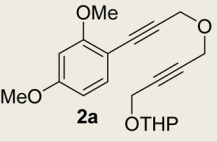
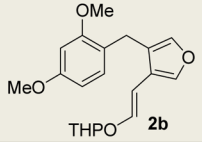
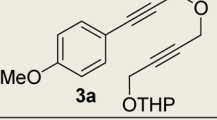
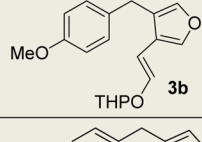
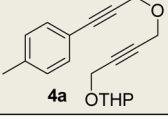
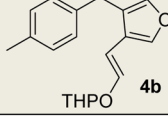
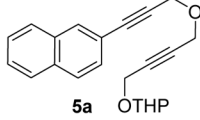
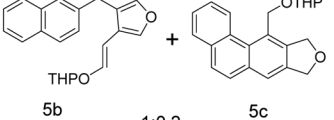
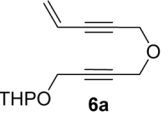
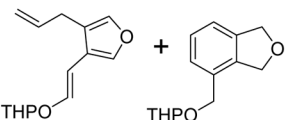
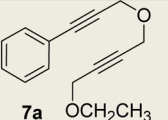
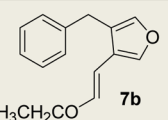
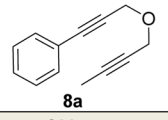
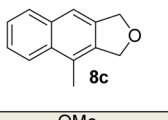
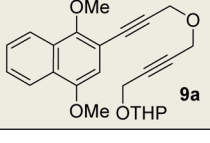
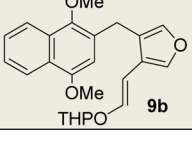
column chromatography (Si-gel), afforded the products. The results are shown in Table 1.

A thorough analysis of the results revealed several interesting outcomes. For phenyl or substituted phenyl ethers, the reaction followed only the 1,5-shift pathway. The presence of acetal/ethereal oxygen at the other arm plays an important role as a replacement with the simple methyl forcing the reaction to proceed entirely through the GB pathway. Another interesting aspect is in the case of naphthalene and vinyl substituted propargyl ethers. In these cases, both GB and 1,5-H shift products were produced in different ratios. This validates our assertion that lesser sacrifice of aromaticity/delocalization energy during self-quenching of the diradical via the GB pathway may allow the GB product to be formed. This is what was observed in the naphthalene system, which has less resonance energy per benzene ring as compared to only phenyl, thus allowing GB product to be formed, although in a lesser amount (ratio of 1,5-H shift product and GB product was 1:0.2) as compared to no GB product in the case of phenyl-based systems. For the vinyl system, no such issue arises, and hence, the GB product became the predominant product.

Double bond fixation also played an important role in deciding the favored pathway. This is exemplified by the earlier reported isolation of only the 1,5-H shift product from the 1,4-dimethoxy naphthyl substituted ether 9a. In naphthalene, there is nonequivalency of bond order due to partial bond fixation, which gives less double bond character to the C2–C3 bond.

The structures of the various products were confirmed by NMR and mass spectroscopic data analysis. For the 3,4-disubstituted furan derivatives, the geometry of the double bond in the initially formed product was found to be *E* (*trans*) ($J = 12.6$ Hz) which, however, got converted into the *Z* (*cis*) form ($J = 6.6$ Hz) upon keeping in CDCl₃ (for spectra, see the Supporting Information). This isomerization generally took 5–6 days for completion; however, in the case of dimethoxy derivative 2b, the isomerization happened during chromatographic purification. This *E*-to-*Z* isomerization at room temperature clearly indicated higher stability for the *Z* isomer! This is quite unprecedented, and we believe that the *Z* form achieves an extra stability via a C–H⋯O hydrogen bond

Table 1. Results of Base Treatment of Various Propargyl Ethers^a

Entry	Reactant	Product	Yield (%)
1	 1a	 1b	80
2	 2a	 2b	70
3	 3a	 3b	75
4	 4a	 4b	80
5	 5a	 5b + 5c 1:0.2	70
6	 6a	 6b + 6c 1:3.18	72
7	 7a	 7b	85
8	 8a	 8c	65
9	 9a	 9b	50

^aReaction conditions: KO^tBu, dry DMSO, rt, 1 h.

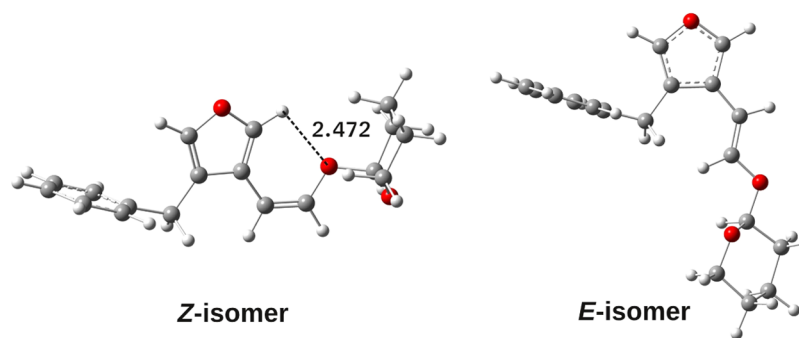


Figure 2. Energy minimized structure [BP86-(D3-BJ)/def2-SVP] of **1b** in Z and E configurations. The Z configuration is more stable than the E configuration by $\Delta E = 3.9 \text{ kcal mol}^{-1}$ ($\Delta G_{298} = 2.4 \text{ kcal mol}^{-1}$). The distance is in angstroms (Å).

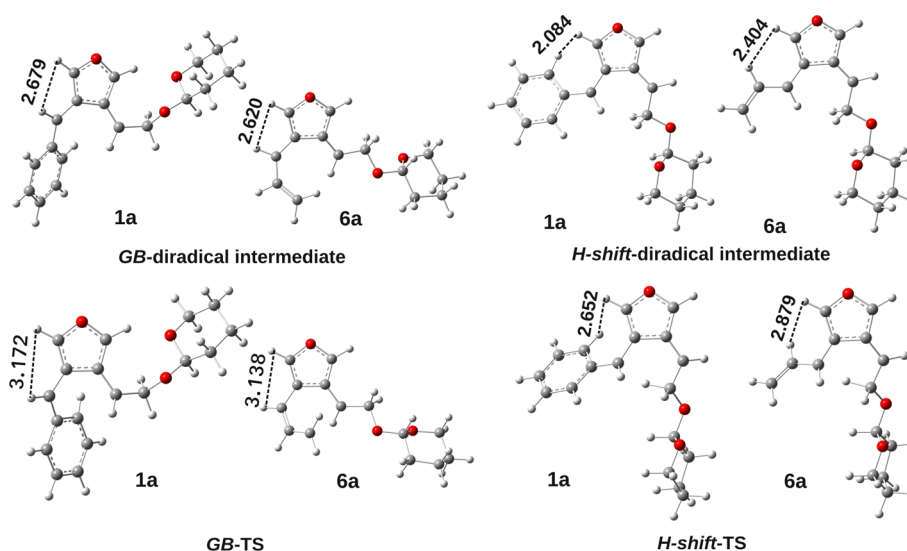


Figure 3. Optimized structure [BP86-(D3-BJ)/def2-SVP] of diradical intermediates and TS's of GB cyclization and 1,5-H-shift for **1a** and **6a**. The distances are in angstroms (Å).

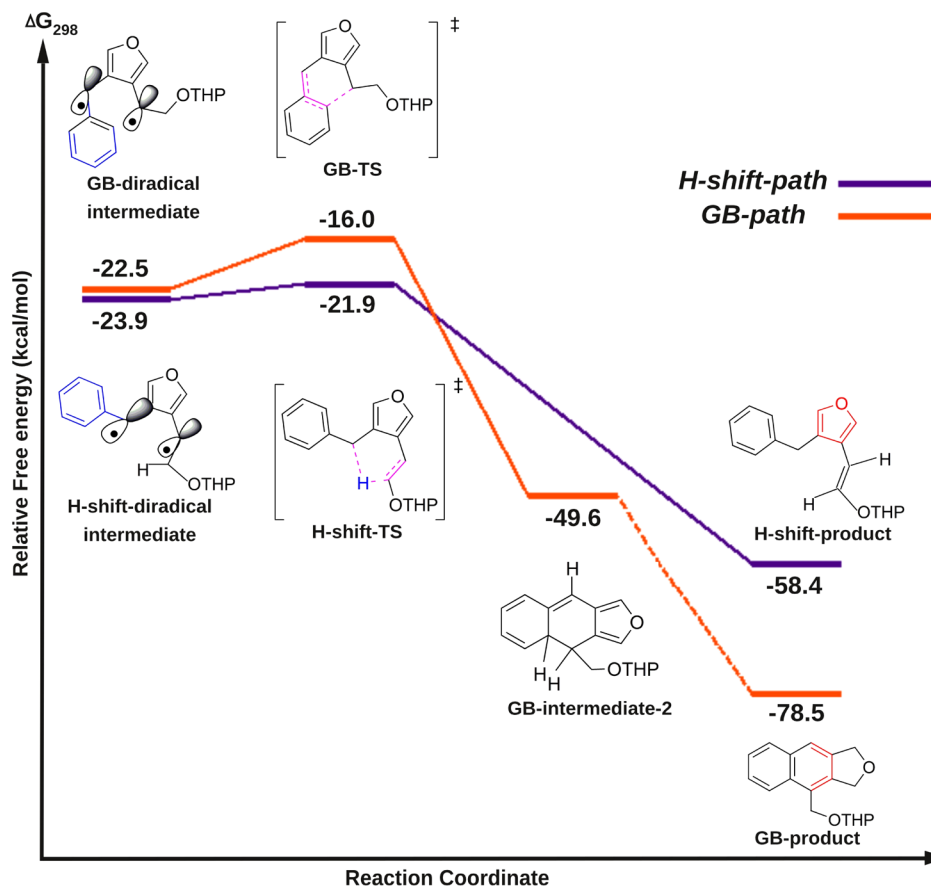


Figure 4. Reaction profile for later stages of 1,5-H shift and GB cyclization for **1a**. Relative free energies [BP86-(D3-BJ)/def2-SVP] are given in kcal mol⁻¹.

involving the furan C2–H. It may be pointed out that there is plenty of computational evidence regarding the existence of such a H-bond.⁹ We have also done energy minimization of the two isomers which, too, indicated the presence of an intramolecular H-bond involving furan H-2 (Figure 2). ¹H NMR taken separately in CDCl₃ and then in *d*₆-DMSO showed a slight upfield shift ($\Delta\delta \approx 0.1$) of the furan H-2 in the *Z*

isomer (for spectra, see the Supporting Information). On the other hand, all other furan hydrogens (H-2 in *E* isomer and H-5 of both *E* and *Z* isomers) showed a downfield shift of $\Delta\delta > 0.2$, indicating the possibility of involvement of H-2 in the *Z* isomer in intramolecular H-bonding. Petrova et al.¹⁰ in their study of conformations of 1,4-dihydropyridine derivatives have shown an upfield shift (CDCl₃ vs *d*₆-DMSO) of hydrogens involved in

similar intramolecular C–H...O bonding. It may be mentioned here that Schmittel et al.¹¹ in a recent paper have reported formation of both *E* and *Z* isomers in thermal Garratt–Braverman/[1,5]-H shift of an ene-diallene system and observed (both experimentally and also based on computations) a nonstatistical dynamics. In our case, the reaction always led to the *E* isomer as the exclusive product, which isomerized to the *Z* form upon keeping in solution or during chromatographic purification.

We have also studied the mechanism of GB cyclization and 1,5-H shift using DFT calculations. The first cyclization of bis-allenyl ether yields a diradical intermediate that undergoes self-quenching, leading to the products (furans via 1,5-H shift and phthalans via GB). Although we have mapped the entire reaction pathway starting from the bis-allene, this discussion is restricted to the diradical self-quenching step. The relative activation energies for the two self-quenching processes should determine the outcome of the reaction. This assumption is possibly justified as both the products originated from the same diradical intermediate. It is true that 1,5-H shift and the GB process involve different conformers of the diradical intermediate. However, the computed energy difference between reacting conformers has been found to be much less in comparison to the corresponding activation energies, leading to the products (except for the olefinic substrate **6a**). This indicated rapid equilibration between the conformers and hence the applicability of the Curtin–Hammett principle.¹² The reason for the higher difference between the two reacting conformers in the case of **6a** may be attributed to the lower van der Waals interaction between the olefin H and furan H-5 as compared to the aryl derivatives (Figure 3). The same trend is also reflected in the TS that resembles the diradical intermediate. The reaction profile for later stages of 1,5-H shift and GB cyclization for substrate **1a** is shown as a representative example (Figure 4).

The computed activation energies are shown in Table 2, which clearly indicated that, for the phenyl substituted systems

Table 2. Computational Results [BP86-(D3-BJ)/def2-SVP]: The Activation Energy (ΔG^\ddagger), Energy Difference between the Reactive Diradical Intermediates ($\Delta\Delta G = \Delta G_{\text{GB}} - \Delta G_{\text{H-shift}}$), and Experimental Product Ratio Are Given^a

Substrate	Reaction type	Activation free energy (ΔG^\ddagger) (kcal mol ⁻¹)	Relative Free energy difference ($\Delta\Delta G$) between the reactive conformers (diradical intermediates) for GB and H-shift processes ($\Delta\Delta G = \Delta G_{\text{GB}} - \Delta G_{\text{H-shift}}$) (kcal mol ⁻¹)	Product Ratio (H-Shift : GB)
1a	H-shift	2.1	1.4	1:0
	GB	6.5		
2a	H-shift	3.2	1.9	1:0
	GB	7.2		
3a	H-shift	3.1	1.3	1:0
	GB	7.7		
5a	H-shift	3.9	1.4	1:0.2
	GB	4.0		
6a	H-shift	5.7	5.2	1:3.18
	GB	4.2		

^aFree energies were calculated at 298 K. All energy values are in kcal mol⁻¹.

(**1a–3a**), the two activation energies (GB and H-shift) differ by more than 2 kcal mol⁻¹, with the GB process having higher activation energy. These systems thus preferred to follow the 1,5-H shift pathway. For the naphthalene system **5a**, this difference is less than 1 kcal mol⁻¹, and hence, both the products were formed with 1,5-H shift showing a higher preference. For the vinyl system, the activation energy for the GB process is less than the 1,5-H shift pathway, thus making the GB process the predominant reaction. In the case of the methyl substituted propargyl ether, the stronger C–H bond as compared to the ethereal system (like OTHP derivative) disfavored the 1,5-H shift. In fact, the calculated C–H bond energy (Scheme 4) for an ethereal system (94.2 kcal mol⁻¹) is lower than the corresponding bond energy for methyl substituted propargyl ether (107.2 kcal mol⁻¹).

In conclusion, we have succeeded in developing a general route to 3,4-disubstituted furans by successfully shifting the reactivity of bis-propargyl ethers toward the 1,5-H shift pathway from the usual GB mode. The parameters controlling this interplay of reactivity have also been identified and rationalized by DFT-based computations. Future studies will aim toward exploring the synthetic utility of the furan derivatives and also carrying out a more elaborate study on the *E*-to-*Z* isomerization.

EXPERIMENTAL SECTION

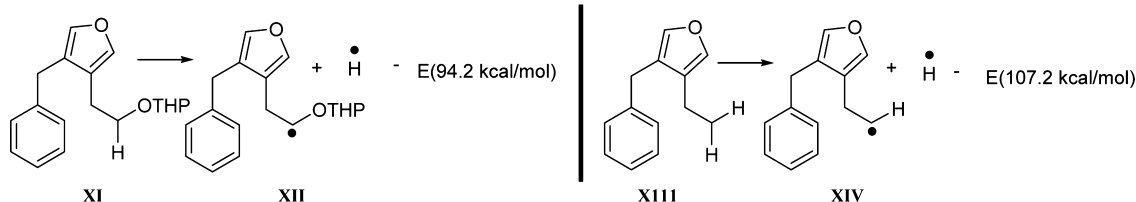
All ¹H NMR and ¹³C NMR spectra were obtained with 200, 400, and 600 MHz NMR instruments in CDCl₃ unless mentioned otherwise. The following abbreviations are used to describe peak patterns where appropriate: s = singlet, d = doublet, t = triplet, q = quartet, m = multiplet, app. = apparently, and b = broad signal. All coupling constants (*J*) are given in Hz. Mass spectra were recorded in ESI+ mode (ion trap). IR spectra were recorded as thin films, and bands are expressed in cm⁻¹.

All the dry solvents used for reactions were purified according to the standard protocols. Dimethyl sulfoxide (DMSO), *N,N*-dimethylformamide (DMF), and triethylamine (Et₃N) were distilled from calcium hydride. All the solvents for column chromatography were distilled prior to use. In most of the column chromatographic purifications, ethyl acetate (EA/EtOAc) and petroleum ether (PE) of boiling range 60–80 °C were used as eluents. Columns were prepared with silica gel (Si-gel, 60–120 and 230–400 mesh, SRL).

General Procedure for O-Propargylation: Synthesis of Compounds (1a–8a). To an ice-cold solution of alcohol (1 mmol) in dry DMF (10 mL) was added NaH (2 equiv, 60% suspension in mineral oil), and the solution was stirred for 30 min at ice-cold temperature under a N₂ atmosphere. After the alkoxide was generated, the respective propargyl bromides (ethyl iodide in the case of **7a**) (1.0 equiv) diluted with dry DMF (5 mL) were added dropwise by maintaining the ice-cold temperature, and the mixture was stirred for 1 h. It was then quenched with aqueous NH₄Cl and partitioned between ethyl acetate and water. The organic layer was washed with brine solution, and the combined organic layer was dried with anhydrous sodium sulfate. The solvent was removed, and the crude residue was purified by column chromatography (Si-gel, petroleum ether–ethyl acetate mixture as eluent).

Preparation of (6a) via Sonogashira Coupling. To a degassed solution of **16** (1 mmol) and vinyl bromide (4 equiv) in dry Et₃N (10 mL) were added PdCl₂(PPh₃)₂ (3 mol %) and CuI (20 mol %) under an inert atmosphere, and the mixture was allowed to stir at room temperature for 18 h. The mixture was then poured to ethyl acetate, and the organic layer was washed with a saturated solution of NH₄Cl and brine. The ethyl acetate layer was then dried over anhydrous sodium sulfate and evaporated, and the purified product was obtained via column chromatography by using hexane–ethyl acetate as eluent.

Spectral Data of Cyclization Products (for 9a, see ref 3d). 2-[4-(3-Phenyl-prop-2-ynoxy)-but-2-ynoxy]-tetrahydro-pyran (**1a**).

Scheme 4. Calculation of C–H Bond Energy from the Optimized Geometries [BP86-(D3-BJ)/def2-SVP]^a

^aHere, the energies are electronic energy. The optimized geometries are included in the SI.

State: yellow oil; **yield:** 227 mg, 80%; IR (neat) ν_{\max} 2927, 2855, 2230, 1611, 1575, 1503, 1210, 1024, 752 cm^{-1} ; ¹H NMR (400 MHz, Chloroform-*d*) δ 7.45–7.43 (m, 2H), 7.32–7.26 (m, 3H), 4.82 (bs, 1H), 4.47 (s, 2H), 4.36 (s, 2H), 4.36–4.26 (m, 2H), 3.86–3.81 (m, 1H), 3.55–3.52 (m, 1H), 1.84–1.54 (m, 6H); ¹³C NMR (50 MHz, Chloroform-*d*) δ 131.8, 128.5, 128.3, 122.5, 96.8, 86.8, 84.3, 83.0, 81.3, 62.0, 57.3, 56.9, 54.3, 30.2, 25.4, 19.0. HRMS: Calcd for $\text{C}_{18}\text{H}_{21}\text{O}_3^+$ [$\text{M} + \text{H}$]⁺ 285.1491 found 285.1494.

2-[4-[3-(2,4-Dimethoxy-phenyl)-prop-2-ynyloxy]-but-2-ynyloxy]-tetrahydro-pyran (2a). **State:** yellow oil; **yield:** 265 mg, 77%; IR (neat) ν_{\max} 2934, 2876, 2231, 1623, 1564, 1034, 750 cm^{-1} ; ¹H NMR (400 MHz, Chloroform-*d*) δ 7.32 (d, $J = 8.0$ Hz, 1H), 6.43–6.41 (m, 2H), 4.81 (t, $J = 3.2$ Hz, 1H), 4.49 (s, 2H), 4.36 (s, 2H), 4.32–4.25 (m, 2H), 3.83 (s, 3H), 3.81 (s, 3H), 3.86–3.79 (m, 1H), 3.54–3.51 (m, 1H), 1.83–1.52 (m, 6H); ¹³C NMR (50 MHz, Chloroform-*d*) δ 161.6, 161.5, 134.8, 104.9, 104.3, 98.5, 97.0, 87.0, 83.3, 82.9, 81.7, 62.2, 57.9, 56.9, 55.9, 55.6, 54.5, 30.4, 25.5, 19.2. HRMS: Calcd for $\text{C}_{20}\text{H}_{25}\text{O}_5^+$ [$\text{M} + \text{H}$]⁺ 345.1702 found 345.1705.

2-[4-[3-(4-Methoxy-phenyl)-prop-2-ynyloxy]-but-2-ynyloxy]-tetrahydro-pyran (3a). **State:** yellow oil; **yield:** 235 mg, 75%; IR (neat) ν_{\max} 2977, 2875, 1576, 2231, 1613, 1045, 754 cm^{-1} ; ¹H NMR (400 MHz, Chloroform-*d*) δ 7.37 (d, $J = 8.8$ Hz, 2H), 6.82 (d, $J = 8.8$ Hz, 2H), 4.81 (t, $J = 3.6$ Hz, 1H), 4.45–4.25 (m, 6H), 3.86–3.79 (m, 4H), 3.54–3.50 (m, 1H), 1.83–1.51 (m, 6H); ¹³C NMR (50 MHz, Chloroform-*d*) δ 159.8, 133.3, 114.5, 113.9, 96.8, 86.8, 82.9, 82.8, 81.3, 61.9, 57.4, 56.8, 55.2, 54.2, 30.2, 25.3, 19.0. HRMS: Calcd for $\text{C}_{19}\text{H}_{23}\text{O}_4^+$ [$\text{M} + \text{H}$]⁺ 315.1596 found 315.1597.

2-[4-[3-(*p*-Tolyl-prop-2-ynyloxy)-but-2-ynyloxy]-tetrahydro-pyran (4a). **State:** yellow oil; **yield:** 247 mg, 83%; IR (neat) ν_{\max} 3100, 2855, 1564, 2231, 1632, 1025, 765 cm^{-1} ; ¹H NMR (400 MHz, Chloroform-*d*) δ 7.29 (d, $J = 7.2$ Hz, 2H), 7.05 (d, $J = 6.8$ Hz, 2H), 4.77 (bs, 1H), 4.40 (s, 2H), 4.30 (s, 2H), 4.30–4.21 (m, 2H), 3.78–3.76 (m, 1H), 3.49–3.47 (m, 1H), 2.28 (s, 3H), 1.77–1.48 (m, 6H); ¹³C NMR (100 MHz, Chloroform-*d*) δ 138.8, 131.9, 129.2, 119.6, 97.0, 87.1, 83.8, 83.2, 81.5, 62.1, 57.5, 57.0, 54.4, 30.4, 25.6, 21.6, 19.2. HRMS: Calcd for $\text{C}_{19}\text{H}_{23}\text{O}_3^+$ [$\text{M} + \text{H}$]⁺ 299.1647 found 299.1643.

2-[4-[3-(*n*-Naphthalen-2-yl-prop-2-ynyloxy)-but-2-ynyloxy]-tetrahydro-pyran (5a). **State:** yellow oil; **yield:** 243 mg, 73%; IR (neat) ν_{\max} 3123, 2937, 2876, 2234, 1506, 1617, 1027, 765 cm^{-1} ; ¹H NMR (600 MHz, Chloroform-*d*) δ 8.00 (s, 1H), 7.83–7.79 (m, 3H), 7.52–7.49 (m, 3H), 4.86 (t, $J = 3.6$ Hz, 1H), 4.55 (s, 2H), 4.44 (s, 2H), 4.43–4.31 (m, 2H), 3.89–3.85 (m, 1H), 3.58–3.55 (m, 1H), 1.88–1.56 (m, 6H); ¹³C NMR (50 MHz, Chloroform-*d*) δ 133.0, 132.9, 131.9, 128.5, 128.1, 127.9, 126.9, 126.7, 119.8, 97.0, 87.2, 84.7, 83.2, 81.4, 62.1, 57.5, 57.1, 54.4, 30.3, 25.5, 19.2. HRMS: Calcd for $\text{C}_{22}\text{H}_{23}\text{O}_3^+$ [$\text{M} + \text{H}$]⁺ 335.1647 found 335.1647.

2-[4-(3-Pent-4-en-2-ynyloxy)-but-2-ynyloxy]-tetrahydro-pyran (6a). **State:** yellow oil; **yield:** 168 mg, 72%; IR (neat) ν_{\max} 2937, 2876, 2234, 1523, 1623, 1025, 745 cm^{-1} ; ¹H NMR (400 MHz, Chloroform-*d*) δ 5.83 (dd, $J = 11.8$ Hz, 7.2 Hz, 1H), 5.68 (dd, $J = 11.8$ Hz, 1.2 Hz, 1H), 5.52 (dd, $J = 7.4$ Hz, 1.2 Hz, 1H), 4.82 (t, $J = 2.0$ Hz, 1H), 4.38 (s, 2H), 4.37–4.27 (m, 4H), 3.87–3.83 (m, 1H), 3.57–3.53 (m, 1H), 1.88–1.55 (m, 6H); ¹³C NMR (50 MHz, Chloroform-*d*) δ 127.8, 116.6, 97.0, 85.5, 85.0, 83.1, 81.3, 62.1, 57.3, 57.0, 54.4, 30.3, 25.5, 19.1. HRMS: Calcd for $\text{C}_{14}\text{H}_{19}\text{O}_3^+$ [$\text{M} + \text{H}$]⁺ 235.1334 found 235.1332.

[3-(4-Ethoxy-but-2-ynyloxy)-prop-1-ynyl]-benzene (7a). **State:** yellow oil; **yield:** 198 mg, 87%; IR (neat) ν_{\max} 3069, 2985, 2852, 2251,

1731, 1604, 1495, 1088, 887, 761, 694 cm^{-1} ; ¹H NMR (400 MHz, Chloroform-*d*) δ 7.45 (m, 2H), 7.32–7.31 (bm, 3H), 4.47 (s, 2H), 4.36 (s, 2H), 4.20 (s, 2H), 3.57 (dd, $J = 7.2$ Hz, 6.8 Hz, 2H), 1.23 (appt, $J = 7.2$ Hz, 3H); ¹³C NMR (50 MHz, Chloroform-*d*) δ 131.8, 128.5, 128.3, 122.5, 86.8, 84.3, 83.2, 81.3, 65.5, 58.0, 57.3, 56.9, 15.0. HRMS: Calcd for $\text{C}_{13}\text{H}_{17}\text{O}_2^+$ [$\text{M} + \text{H}$]⁺ 229.1229 found 229.1223.

(3-But-2-ynyloxy-prop-1-ynyl)-benzene (8a). **State:** yellow oil; **yield:** 154 mg, 84%; IR (neat) ν_{\max} 3066, 2960, 2932, 2859, 2230, 1963, 1611, 1499, 1362, 1132, 926, 894, 764, 698 cm^{-1} ; ¹H NMR (400 MHz, Chloroform-*d*) δ 7.46–7.45 (bm, 2H), 7.32–7.31 (bm, 3H), 4.46 (s, 2H), 4.28 (apps, 2H), 1.88 (s, 3H); ¹³C NMR (50 MHz, Chloroform-*d*) δ 131.8, 128.5, 128.3, 122.6, 86.5, 84.6, 83.2, 74.5, 57.2, 57.1, 3.6. HRMS: Calcd for $\text{C}_{13}\text{H}_{13}\text{O}^+$ [$\text{M} + \text{H}$]⁺ 185.0966 found 185.0965.

General Procedure for Furan Ring Formation: Synthesis of Compounds (1b–8c). To an ice-cold solution of the ethers 1a–9a (0.2 mmol) in dry DMSO (5 mL) was added KO^tBu (1.2 equiv), and the reaction was allowed to stir at room temperature for 1 h. It was then quenched with NH₄Cl solution and extracted with ethyl acetate. The organic layer was dried over anhydrous sodium sulfate and evaporated to get the crude product, which was purified by column chromatography with hexane–ethyl acetate mixture as eluent.

2-[2-(4-Benzyl-furan-3-yl)-vinyloxy]-tetrahydro-pyran (1b). **State:** yellow oil; **yield:** 45 mg, 80%; IR (neat) ν_{\max} 2954, 2874, 2857, 1660, 1530, 1234, 1178, 1050, 767 cm^{-1} ; ¹H NMR (600 MHz, Chloroform-*d*) δ 7.39 (s, 1H), 7.34–7.31 (m, 2H), 7.28–7.23 (m, 3H), 7.08 (s, 1H), 6.73 (d, $J = 12.6$ Hz, 1H), 5.80 (d, $J = 13.2$ Hz, 1H), 4.96 (app s, 1H), 3.86–3.83 (m, 1H), 3.81 (s, 2H), 3.59–3.57 (m, 1H), 1.90–1.57 (m, 6H); ¹³C NMR (150 MHz, Chloroform-*d*) δ 144.5, 141.0, 139.7, 138.4, 128.6, 128.4, 126.1, 123.1, 121.1, 98.7, 98.4, 62.0, 30.3, 29.6, 25.1, 18.6. HRMS: Calcd for $\text{C}_{18}\text{H}_{21}\text{O}_3^+$ [$\text{M} + \text{H}$]⁺ 285.1491 found 285.1495.

2-[2-[4-(2,4-Dimethoxy-benzyl)-furan-3-yl]-vinyloxy]-tetrahydro-pyran (2b). **State:** yellow oil; **yield:** 48 mg, 70%; IR (neat) ν_{\max} 2989, 2945, 2867, 1664, 1567, 1357, 1209, 1098, 756 cm^{-1} ; ¹H NMR (600 MHz, Chloroform-*d*) δ 7.90 (s, 1H), 7.10 (s, 1H), 6.97 (d, $J = 8.4$ Hz, 1H), 6.49 (d, $J = 2.4$ Hz, 1H), 6.44 (d, $J = 6.6$ Hz, 1H), 6.42 (dd, $J = 7.8$ Hz, 2.4 Hz, 1H), 5.19 (d, $J = 6.6$ Hz, 1H), 5.13 (app t, $J = 2.4$ Hz, 1H), 3.84 (s, 3H), 3.81 (s, 3H), 3.70 (s, 2H), 3.71–3.70 (m, 1H), 3.62–3.60 (m, 1H), 1.95–1.69 (m, 6H); ¹³C NMR (150 MHz, Chloroform-*d*) δ 159.3, 157.9, 142.5, 142.0, 139.7, 129.9, 122.4, 120.8, 119.6, 103.8, 98.8, 98.3, 96.2, 61.6, 55.4, 55.3, 29.6, 25.1, 22.7, 18.6. HRMS: Calcd for $\text{C}_{20}\text{H}_{24}\text{NaO}_5^+$ [$\text{M} + \text{Na}$]⁺ 367.1521 found 367.1541.

2-[4-[3-(4-Methoxy-phenyl)-prop-2-ynyloxy]-but-2-ynyloxy]-tetrahydro-pyran (3b). **State:** yellow oil; **yield:** 47 mg, 75%; IR (neat) ν_{\max} 2954, 2876, 1667, 1530, 1359, 1213, 1095, 789 cm^{-1} ; ¹H NMR (400 MHz, Chloroform-*d*) δ 7.34 (s, 1H), 7.12 (d, $J = 8.0$ Hz, 2H), 7.02 (s, 1H), 6.83 (d, $J = 8.0$ Hz, 2H), 6.70 (d, $J = 12.8$ Hz, 1H), 5.75 (d, $J = 12.8$ Hz, 1H), 4.93 (app s, 1H), 3.84–3.82 (m, 1H), 3.79 (s, 3H), 3.70 (s, 2H), 3.56–3.54 (m, 1H), 1.87–1.53 (m, 6H); ¹³C NMR (100 MHz, Chloroform-*d*) δ 158.0, 144.4, 140.9, 138.4, 131.7, 129.5, 123.6, 121.0, 113.8, 98.8, 98.4, 62.0, 55.2, 29.6, 29.5, 25.1, 18.6. HRMS: Calcd for $\text{C}_{19}\text{H}_{23}\text{O}_4^+$ [$\text{M} + \text{H}$]⁺ 315.1596 found 315.1591.

2-[2-[4-(4-Methyl-benzyl)-furan-3-yl]-vinyloxy]-tetrahydro-pyran (4b). **State:** yellow oil; **yield:** 47 mg, 80%; IR (neat) ν_{\max} 2948, 2929, 2876, 2854, 1664, 1520, 1464, 1357, 1206, 1169, 1090, 786, 745 cm^{-1} ; ¹H NMR (400 MHz, Chloroform-*d*) δ 7.35 (s, 1H), 7.11 (s, 4H), 7.04 (s, 1H), 6.71 (d, $J = 12.8$ Hz, 1H), 5.77 (d, $J = 12.8$ Hz, 1H), 4.96 (app

s, 1H), 3.85–3.81 (m, 1H), 3.73 (s, 2H), 3.57–3.55 (m, 1H), 2.33 (s, 3H), 1.75–1.57 (m, 6H); ¹³C NMR (100 MHz, Chloroform-*d*) δ 144.6, 141.1, 138.5, 136.8, 135.8, 129.3, 128.7, 123.6, 121.2, 99.0, 98.6, 62.2, 30.1, 29.9, 25.3, 21.2, 18.8. HRMS: Calcd for C₁₉H₂₂NaO₃⁺ [M + Na]⁺ 321.1467 found 321.1467.

2-[2-(4-Naphthalen-2-ylmethyl-furan-3-yl)-vinyl]oxy]-tetrahydro-pyran (5b). State: yellow oil; yield: 39 mg, 58%; IR (neat) ν_{\max} 2950, 2786, 1669, 1465, 1208, 1178, 1098, 745 cm⁻¹; ¹H NMR (600 MHz, DMSO-*d*₆) δ 7.87–7.81 (m, 3H), 7.68 (s, 1H), 7.65 (s, 1H), 7.49–7.44 (m, 3H), 7.38 (d, *J* = 8.4 Hz, 1H), 6.77 (d, *J* = 12.6 Hz, 1H), 5.64 (d, *J* = 12.6 Hz, 1H), 4.91 (app s, 1H), 3.92 (s, 2H), 3.59–3.55 (m, 1H), 3.38–3.34 (m, 1H), 1.67–1.40 (m, 6H); ¹³C NMR (150 MHz, Chloroform-*d*) δ 144.5, 141.1, 138.4, 137.2, 133.6, 132.2, 128.0, 127.6, 127.3, 126.8, 125.9, 125.3, 123.0, 121.1, 98.7, 98.3, 61.9, 30.5, 29.6, 25.0, 18.6. HRMS: Calcd for C₂₂H₂₂NaO₃⁺ [M + Na]⁺ 357.1467 found 357.1471.

7-((Tetrahydro-2H-pyran-2-yloxy)methyl)-8,10-dihydrophenanthro[2,3-*cf*]furan (5c). State: yellow oil; yield: 9 mg, 13%; IR (neat) ν_{\max} 3069, 2965, 2867, 1645, 1475, 1145, 755 cm⁻¹; ¹H NMR (600 MHz, Chloroform-*d*) δ 8.91 (d, *J* = 9.0 Hz, 1H), 7.93 (d, *J* = 9.6 Hz, 1H), 7.74–7.71 (m, 3H), 7.64–7.63 (m, 2H), 5.50 (app s, 2H), 5.38–5.35 (m, 3H), 4.99–4.96 (m, 2H), 4.12–4.08 (m, 1H), 3.74–3.70 (m, 1H), 2.07–1.64 (m, 6H); ¹³C NMR (150 MHz, Chloroform-*d*) δ 141.4, 139.3, 137.8, 133.7, 133.3, 130.5, 130.3, 128.4, 128.0, 127.4, 127.1, 126.3, 125.9, 120.8, 98.9, 73.6, 73.5, 67.7, 62.6, 30.2, 25.5, 19.4. HRMS: Calcd for C₂₂H₂₂NaO₃⁺ [M + Na]⁺ 357.1467 found 357.1469.

2-[2-(4-Allyl-furan-3-yl)-vinyl]oxy]-tetrahydro-pyran (6b). State: yellow oil; yield: 9 mg, 18%; IR (neat) ν_{\max} 2947, 2875, 1667, 1525, 1234, 1095, 734 cm⁻¹; ¹H NMR (400 MHz, Chloroform-*d*) δ 7.36 (s, 1H), 7.34 (s, 1H), 6.77 (d, *J* = 12.8 Hz, 1H), 6.60 (d, *J* = 8.0 Hz, 1H), 6.13 (d, *J* = 11.2 Hz, 1H), 5.86–5.78 (m, 2H), 5.02–4.91 (m, 2H), 4.73 (app s, 1H), 3.90–3.84 (m, 1H), 3.60–3.58 (m, 1H), 2.07–1.67 (m, 6H); ¹³C NMR (150 MHz, Chloroform-*d*) δ 137.7, 137.6, 136.3, 126.0, 118.4, 114.1, 99.0, 98.9, 62.2, 31.9, 30.7, 30.6, 22.7, 19.5. HRMS: Calcd for C₁₄H₁₈NaO₃⁺ [M + Na]⁺ 257.1154 found 257.1154.

4-(Tetrahydro-pyran-2-yloxymethyl)-1,3-dihydro-isobenzofuran (6c). State: yellow oil; yield: 25 mg, 55%; IR (neat) ν_{\max} 2956, 2935, 2856, 1668, 1465, 1205, 1093, 786 cm⁻¹; ¹H NMR (600 MHz, Chloroform-*d*) δ 7.29–7.24 (m, 2H), 7.19–7.18 (d, *J* = 7.2 Hz, 1H), 5.20 (app s, 2H), 5.14 (s, 2H), 4.78 (d, *J* = 12.6 Hz, 1H), 4.71 (t, *J* = 3.0 Hz, 1H), 4.47 (d, *J* = 12.6 Hz, 1H), 3.93–3.89 (m, 1H), 3.59–3.56 (m, 1H), 1.9–1.56 (m, 6H); ¹³C NMR (150 MHz, Chloroform-*d*) δ 139.5, 137.8, 131.9, 127.5, 126.5, 120.1, 97.9, 73.5, 73.0, 67.3, 62.0, 30.5, 25.4, 19.2. HRMS: Calcd for C₁₄H₁₈NaO₃⁺ [M + Na]⁺ 257.1154 found 257.1154.

3-Benzyl-4-(2-ethoxy-vinyl)-furan (7b). State: yellow oil; yield: 39 mg, 85%; IR (neat) ν_{\max} 2987, 2956, 2867, 1669, 1356, 1189, 1067, 755 cm⁻¹; ¹H NMR (600 MHz, Chloroform-*d*) δ 7.35 (s, 1H), 7.33–7.31 (m, 2H), 7.24–7.23 (m, 3H), 7.10 (s, 1H), 6.63 (d, *J* = 12.6 Hz, 1H), 5.46 (d, *J* = 12.6 Hz, 1H), 3.79 (app q, *J* = 8.4 Hz, 4H), 1.29 (dd, *J* = 7.2 Hz, 6.6 Hz, 3H); ¹³C NMR (50 MHz, Chloroform-*d*) δ 147.8, 141.1, 139.9, 138.1, 128.7, 128.6, 126.3, 123.3, 121.6, 95.0, 65.5, 30.4, 14.9. HRMS: Calcd for C₁₅H₁₇O₂⁺ [M + H]⁺ 229.1229 found 229.1213.

4-Methyl-1,3-dihydro-naphtho[2,3-*c*]furan (8c). State: sticky mass; yield: 24 mg, 65%; IR (neat) ν_{\max} 3100, 2986, 2934, 1667, 1523, 1356, 1189, 1098, 785, 747 cm⁻¹; ¹H NMR (600 MHz, Chloroform-*d*) δ 8.02 (d, *J* = 7.2 Hz, 1H), 7.84 (d, *J* = 8.4 Hz, 1H), 7.57 (s, 1H), 7.53–7.47 (m, 2H), 5.28 (s, 2H), 5.27 (s, 2H), 2.58 (s, 3H); ¹³C NMR (150 MHz, Chloroform-*d*) δ 137.4, 136.6, 133.5, 132.1, 128.5, 126.2, 125.5, 125.3, 123.5, 117.3, 73.5, 72.8, 15.4. HRMS: Calcd for C₁₃H₁₃O⁺ [M + H]⁺ 185.0966 found 185.0968.

COMPUTATIONAL DETAILS

All the computations were carried out with the Orca 3.0.3¹³ software package. Geometry optimizations were done in gas phase using Density Functional Theory (DFT) using the BP86¹⁴ functional, and the def2-SVP basis set¹⁵ with the resolution of identity (RI) approximation.¹⁶ Empirical dispersion correction¹⁷ (DFT-D3BJ) was included in all calculations. Unrestricted formalism was used for the

open-shell diradical intermediate. The nature of the stationary point was characterized by vibrational frequency analysis.

ASSOCIATED CONTENT

Supporting Information

The Supporting Information is available free of charge on the ACS Publications website at DOI: 10.1021/acs.joc.5b02246.

Spectral data of all new compounds, copies of NMR (¹H and ¹³C) spectra for all compounds, and computational details (PDF)

AUTHOR INFORMATION

Corresponding Authors

*E-mail: absk@chem.iitkgp.ernet.in (A.B.).

*E-mail: anoop@chem.iitkgp.ernet.in (A.A.).

Author Contributions

[†]Major contributor to the experimental work.

Author Contributions

[‡]Major contributor to the computational work.

Notes

The authors declare no competing financial interest.

ACKNOWLEDGMENTS

A.B. is grateful to CSIR, Govt. of India, for funding (No. 02(0014)/11/EMR-I) and to DST, Govt. of India, for the JC Bose fellowship. J.D. thanks CSIR, Govt. of India, for a research fellowship (NET). E.D. thanks IIT Kharagpur for an institute research fellowship. DST and IIT Kharagpur are also thanked for the funds for 400 MHz (IRPHA program) and 600 MHz facilities, respectively.

REFERENCES

- (1) (a) Basak, A.; Das, S.; Mallick, D.; Jemmis, E. D. *J. Am. Chem. Soc.* **2009**, *131*, 15695. (b) Das, J.; Mukherjee, R.; Basak, A. *J. Org. Chem.* **2014**, *79*, 3789.
- (2) (a) Garratt, P. J.; Neoh, S. B. *J. Am. Chem. Soc.* **1975**, *97*, 3255. (b) Cheng, Y. S. P.; Dominguez, E.; Garratt, P. J.; Neoh, S. B. *Tetrahedron Lett.* **1978**, *19*, 691. (c) Garratt, P. J.; Neoh, S. B. *J. Org. Chem.* **1979**, *44*, 2667. (d) Braverman, S.; Duar, Y. *J. Am. Chem. Soc.* **1990**, *112*, 5830. (e) Braverman, S.; Zafrani, Y.; Gottlieb, H. E. *J. Org. Chem.* **2002**, *67*, 3277. (f) Braverman, S.; Pechenick, T.; Gottlieb, H. E.; Sprecher, M. *J. Am. Chem. Soc.* **2003**, *125*, 14290. (g) Braverman, S.; Pechenick-Azizi, T.; Gottlieb, H.; Sprecher, M. *Synthesis* **2011**, *2011*, 1741.
- (3) (a) Feldman, K. S.; Selfridge, B. R. *Heterocycles* **2010**, *81*, 117. (b) Mondal, S.; Maji, M.; Basak, A. *Tetrahedron Lett.* **2011**, *52*, 1183. (c) Mondal, S.; Mitra, T.; Mukherjee, R.; Addy, P. S.; Basak, A. *Synlett* **2012**, *23*, 2582. (d) Addy, P. S.; Dutta, S.; Biradha, K.; Basak, A. *Tetrahedron Lett.* **2012**, *53*, 19. (e) Mitra, T.; Das, J.; Maji, M.; Das, R.; Das, U. K.; Chattaraj, P. K.; Basak, A. *RSC Adv.* **2013**, *3*, 19844. (f) Mitra, T.; Jana, S.; Pandey, S.; Bhattacharya, P.; Khamrai, U. K.; Anoop, A.; Basak, A. *J. Org. Chem.* **2014**, *79*, 5608.
- (4) (a) Braverman, S.; Segev, D. *J. Am. Chem. Soc.* **1974**, *96*, 1245. (b) Zafrani, Y.; Gottlieb, H. E.; Sprecher, M.; Braverman, S. *J. Org. Chem.* **2005**, *70*, 10166.
- (5) Maji, M.; Mallick, D.; Mondal, S.; Anoop, A.; Bag, S. S.; Basak, A.; Jemmis, E. D. *Org. Lett.* **2011**, *13*, 888.
- (6) Kudoh, T.; Mori, T.; Shirahama, M.; Yamada, M.; Ishikawa, T.; Saito, S.; Kobayashi, H. *J. Am. Chem. Soc.* **2007**, *129*, 4939.
- (7) (a) Yang, Y.; Wong, H. N. C. *J. Chem. Soc., Chem. Commun.* **1992**, 656. (b) Yang, Y.; Wong, H. N. C. *Tetrahedron* **1994**, *50*, 9583.
- (8) Ansell, M. F.; Caton, M. P. L.; North, P. C. *Tetrahedron Lett.* **1981**, *22*, 1727.

- (9) Sánchez-García, E.; Mardjukov, A.; Studentkowski, M.; Montero, L. A.; Sander, W. *J. Phys. Chem. A* **2006**, *110*, 13775.
- (10) Petrova, M.; Muhamadejev, R.; Vigante, B.; Cekavicus, B.; Plotniece, A.; Duburs, G.; Liepinsh, E. *Molecules* **2011**, *16*, 8041.
- (11) Samanta, D.; Rana, A.; Schmittel, M. *J. Org. Chem.* **2014**, *79*, 8435–8439.
- (12) Seeman, J. I. *J. Chem. Educ.* **1986**, *63*, 42.
- (13) Neese, F. *Orca 3.0.3*; Max Planck Institute for Bioinorganic Chemistry: Mülheim/Ruhr, Germany. <https://orcaforum.cec.mpg.de>.
- (14) (a) Becke, A. D. *Phys. Rev. A: At., Mol., Opt. Phys.* **1988**, *38*, 3098. (b) Perdew, J. P. *Phys. Rev. B: Condens. Matter Mater. Phys.* **1986**, *33*, 8822.
- (15) Schäfer, A.; Horn, H.; Ahlrichs, R. *J. Chem. Phys.* **1992**, *97*, 2571.
- (16) Eichkorn, K.; Weigend, F.; Treutler, O.; Ahlrichs, R. *Theor. Chem. Acc.* **1997**, *97*, 119.
- (17) (a) Grimme, S.; Antony, J.; Ehrlich, S.; Krieg, H. *J. Chem. Phys.* **2010**, *132*, 154104. (b) Grimme, S.; Ehrlich, S.; Goerigk, L. *J. Comput. Chem.* **2011**, *32*, 1456.